

*Full Length Research Paper*

# Mineralogy and physico-chemical properties of alluvial clays from far-north region of Cameroon: A tool for an environmental problem

H. Zangué Adjia<sup>1,2,3\*</sup>, F. Villiéras<sup>2,3</sup>, R. Kamga<sup>1</sup> and F. Thomas<sup>2,3</sup>

<sup>1</sup>Département de chimie Appliquée et phénomènes d'interfaces, Ecole Nationale Supérieure des Sciences Agro-industrielles, Université de Ngaoundéré, B.P 455 Ngaoundéré-Cameroon.

<sup>2</sup>Université de Lorraine, L E M, UMR 7569, 15 Avenue du Charmois, B.P. 40. F-54501, Vandoeuvre-Lès-Nancy Cedex.

<sup>3</sup>CNRS, L E M, UMR 7569, 15 Avenue du Charmois, B.P. 40. F-54501, Vandoeuvre-Lès-Nancy Cedex.

Accepted 5 December, 2012

**In a view to evaluate their potential use as adsorbent for wastewater treatment, the mineralogical and physico-chemical properties of alluvial clays from far north region of Cameroon has been determined. Chemical, X- ray diffraction (XRD), Fourier transform infrared spectroscopy (FTIR), scanning electron microscope (SEM) and transmission electron microscopy (TEM) analysis of the alluvial clays reveal that the main mineral present is smectite, kaolinite and quartz. Particle size distribution of the clay is centered around particles of 2, 5 and 30  $\mu\text{m}$  dimension. Cation exchange capacity (CEC) and specific surface area of the raw clay fraction are 62 meq/100 g and 104  $\text{m}^2/\text{g}$  respectively. Those results lie within the values usually found for smectites. Mild acid attack (use of 0.5 M HCl solution) did not induce any noticeable change of clay structure and texture, but the exchangeable cation ( $\text{Ca}^{2+}$ ,  $\text{Na}^+$ ,  $\text{Mg}^{2+}$ ) are removed. It is also observed that  $\text{Fe}^{2+}$  and  $\text{K}^+$  atoms are part of clay lattice. The overall formula of the clay mineral which was established are: smectite,  $[\text{Si}_{3.42}\text{Al}_{0.58}]_{\text{tetra}}[\text{Al}_{0.87}\text{Fe}_{0.96}\text{Mg}_{0.17}]_{\text{octa}}\text{O}_{10}(\text{OH})_2(\text{C}^+)_{0.75}$ ; and kaolinite,  $\text{Si}_2\text{Al}_{1.95}\text{Fe}_{0.05}\text{O}_5(\text{OH})_4$ . Acid activation was attributed to the protonation of negative charge of smectite at low pH and by replacement of  $\text{H}^+$  ion by  $\text{Na}^+$  ion at high pH.**

**Key words:** Alluvial clays, Cameroon, mineralogy, crystal-chemistry, smectites, textural properties.

## INTRODUCTION

Cameroon in the process of growing as a developing country is experiencing major environmental problems related to pollution generated by urbanisation, industries and agriculture. These activities produce higher toxic wastewater which contains organic compounds and heavy metals such as lead, mercury, chromium and copper. This wastewater is rejected in the environment without any treatment (Era-Cameroun, 2002). These waste cause a progressive health problem to human and destruction of the environment (World Bank, 1992). Therefore, low-cost and sustainable methods for wastewater treatment are rapidly needed. Adsorption of undesirable matters on clay seems to be one of those

methods (Robertson et al., 1982; Alther, 1999). Clayey materials are widely used for the removal of solute from solution. Namely crude and activated clay have been used for the adsorption of pigment from vegetable oils (Kamga et al., 2000; Djoufac et al., 2007; Bike et al., 2005), of organic compounds and pesticides from solutions (Davies and Nustrat, 2002, 2003; Worrall et al., 1996; Maqueda and Morillo, 2001) and for dye and of heavy metal removal from solutions (Espantaléon et al., 2003; Shawabkeh and Tutunji, 2003; Yvon et al., 2002). Those adsorption properties of clays are usually attributed to their high porosity, large surface area and high cation exchange capacity (Lumdsen et al., 1995; Wu et al., 1999). However those properties of clays depend strongly on the origin and on the preliminary treatment of the clays.

Cameroon by its geological structure has large deposits

\*Corresponding author. E-mail: henrietteadjia@yahoo.fr.

of clay open to industrial and technological applications (Nguetnkam et al., 2007a; Nguetnkam, 2004). Numerous studies have been carried out on the characterisation, cement and ceramic application of clay from southern region of Cameroon (Pialy et al., 2009; Bitom et al., 2003). In contrast there are very few studies on the mineralogy and use of clays from vertisol of the northern region of Cameroon. None of the above studies are dealing with alluvial clay of the far north region of Cameroon.

The main objective of this study is to investigate the typology of alluvial clayey soil from far north region of Cameroon and to evaluate the effect of mild acid treatment on their properties. This study is part of wide research program aimed at investigating and developing local clays for wastewater treatment and other industrial applications.

## MATERIALS AND METHODS

### Area descriptions and soil samples

The soil samples were taken in a dry river bed situated between the towns of Maroua and Kaélé in the far-north region of Cameroon. The system coordinates of this area is 10°02.883N and 014°23.084E. The climate is tropical-dry, characterized by 7 to 8 months of dry season and 4 to 5 months of wet season. The mean annual rainfall and temperature in the area is 800 mm and 28.5°C, respectively. During the wet season the rivers (locally call Mayo) contain running water while in the dry season there is almost no water. The soil depth during the sampling is 99 cm (Nguetnkam et al., 2007b). The location of the studied soil is shown in Figure 1.

### Extraction of particle size

The soil fraction was pounded in a mortar and then placed in an ultrasound bath for 2 h. The resulting mixture was then sieved over 50 µm mesh sieve. Pure water (MilliQ ultrapure) was used to facilitate the sieving process. The resulting mixture was dried in an oven at 105°C until complete evaporation of water. The solid obtained was treated with 5% hydrogen peroxide solution to eliminate organic matter. Clay fraction (<2 µm) was extracted by sedimentation.

Particle size distribution was obtained using Helos Sympactec type apparatus. For this purposes 1 g of clay sample was introduced in a 50 ml of 0.1% (w/w) (NaPO<sub>3</sub>)<sub>6</sub> solutions. Prior to the particle size analyses, the clay suspension was dispersed by ultrasound for 5 min.

Mild acid activation was carried out by mixing 100 g of clay with 250 ml of HCl 0.5 M (67.5 mMol H<sup>+</sup>) solution, to replace exchangeable cations with H<sup>+</sup> ions without significant alteration of the clay structure. The suspensions were stirred at 60°C for 48 h, using a magnetic stirrer operating at 30 rpm. After cooling at room temperature, the suspensions were filtered and the solid phases were washed several times with pure water until the silver nitrate test for chlorine was negative. The obtained activated clays were then dried at 105°C up to constant weight and the resulting solid was gently pulverized in an agate mortar. Clays fraction studied in this work are the sandy fraction (<50 µm) that is, A50, the clay fraction (<2 µm) that is, A02 and their respective activated samples (A50A and A02A).

The X-ray diffraction (XRD) data were obtained using a D8 Bruker diffractometer with CoK<sub>α1</sub> radiation (λ = 1.789 Å).

Spectra were recorded on oriented and unoriented samples. The detection limit for a given crystalline phase is estimated at around 1% in mass. Ethylene glycol and heat treatments (550°C) were used to provide additional information essential for the identification of clay minerals.

Infrared spectra were recorded using an IFS 55 Bruker Fourier transform IR spectrometer equipped with an MCT detector (6000 to 600 cm<sup>-1</sup>) cooled at 77K and in diffuse reflectance (Harrick attachment) mode. The amount of clay was 70 mg dispersed in 370 mg KBr.

TEM observations were carried out with a Philips CM20 microscope equipped with an EDS detector. Secondary and backscattering SEM observations were carried out on a Hitachi 2500 LB SE microscope equipped with a Kevex Delta EDS spectrometer. SEM was used to assist in the identification of individual accessory minerals incorporated in the clay samples by comparing their morphological characteristics with their elemental compositions.

Chemical analyses were performed on the two clay fractions and their acid treated forms. The major elements were determined by inductively coupled plasma atomic emission spectroscopy (ICP-AES), while trace elements and rare earths elements were determined by inductively coupled plasma mass spectrometry (ICP-MS).

Cationic exchange capacities (CEC) were measured using cobaltihexamine [Co(NH<sub>3</sub>)<sub>6</sub>Cl<sub>3</sub>] as exchangeable ions. The amount of cobaltihexamine fixed by the solid phase was determined from concentration measurements using UV-vis spectroscopy. The displaced cations were determined by atomic absorption spectrometry (Perkin-Elmer 1100B). The equilibrium pH of clay suspensions were determined using a standard LPH 330 T electrode.

Nitrogen adsorption-desorption isotherms at 77K were recorded on a step-by-step automatic home-built set up. Pressures were measured using 0 to 1000 Pa and 0 to 100.000 Pa Baratron-type pressure sensors provided by Edwards. The nitrogen saturation pressure was recorded *in situ* using an independent 0 to 100.000 Pa Baratron-type pressure sensor provided by Edwards. Prior to adsorption, the samples were out gassed overnight at 120°C and under a residual pressure of 0.01 Pa. Nitrogen N55 (purity > 99.9995%) used for experiments was provided by alphasgaz (France). Specific surface areas (SSA) were determined from adsorption data by applying the Brunauer-Emmet-Teller (BET) equation and using 16.3 Å<sup>2</sup> for the cross sectional area of nitrogen. In the present study, the error in the determination of the SSA was estimated as +/- 1 m<sup>2</sup>/g. Micropores volumes and non microporous surface areas were obtained using the t-plot method proposed by De Boer et al. (1996). Pore size distributions were calculated on the desorption branch using the Barrett-Joyner-Halenda method, assuming slit-shaped pores.

The thermal analysis diagrams were obtained on 47 mg of sample with thermo-balance +/- 0.1 mg. The thermogravimetric and differential thermogravimetric (TG and DTG) were obtained with a Toledo 851 thermal analyser (Mettler) at a heating rate of 10°C/min, using air atmosphere, in the temperature range 20 to 1200°C.

## RESULTS AND DISCUSSION

### Extraction yield, particle size distribution and dissolution's behaviour on acid treatment

The extraction yields of A50 fraction (< 50 µm) and A02 clay fraction (< 2 µm) are 67 and 38%, respectively (Table 1). Therefore the sandy fraction, particle size between 2 and 50 µm, represents about 29% of the soil

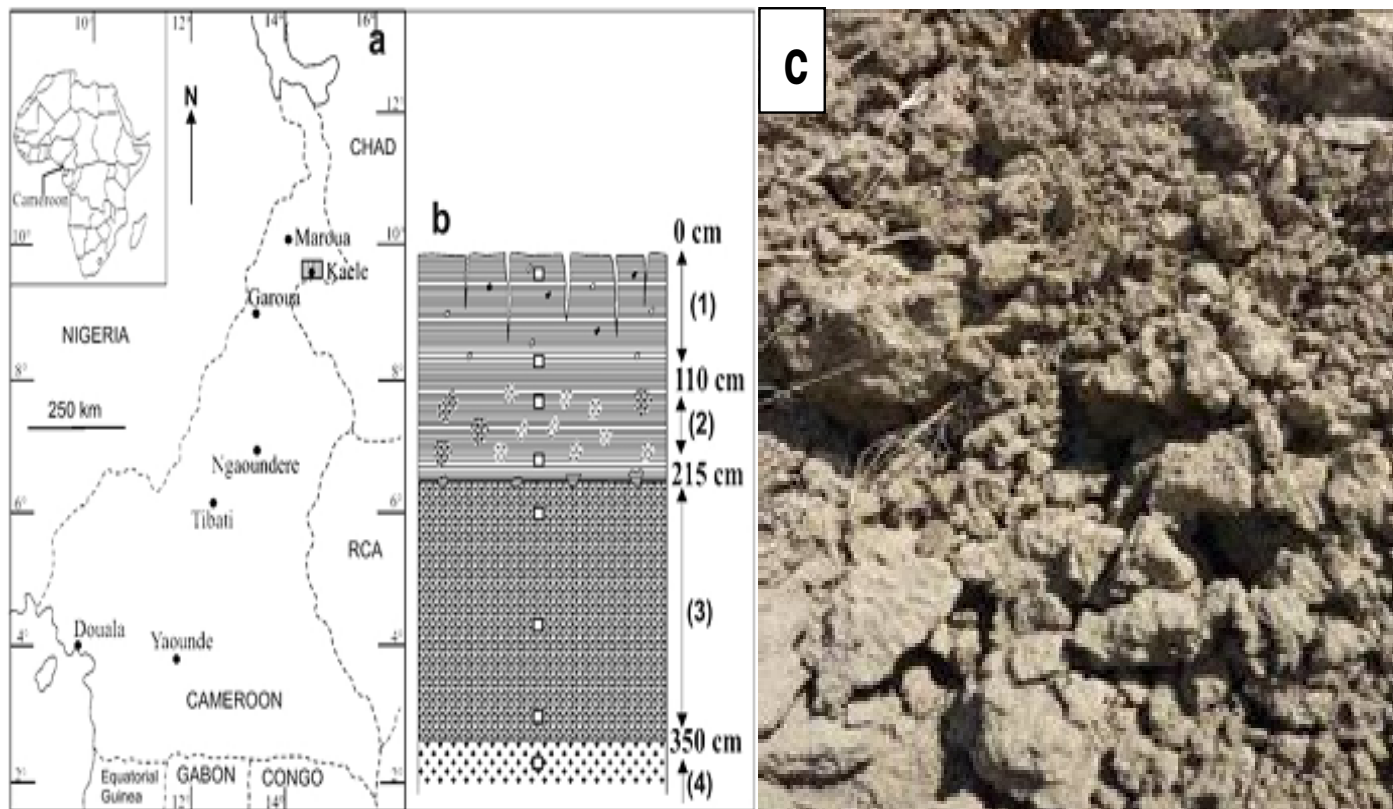


**Figure 1.** (a) Location of the far-North region of Cameroon. (b) Soil profile: (1) dark grey horizon; (2) intermediate horizon; (3) saprolite; (4) granite. Open squares indicate the sources of the soil samples; (c) picture of sample.

**Table 1.** Extraction yield, particle size distribution and dissolution behaviour of sandy and clays fractions.

Sample	Extraction yield (%)	Mean particle size ( $\mu\text{m}$ )	0.5 M HCl residual (%)
Sandy fraction (A50)	$67 \pm 1$	$5.8 \pm 1$	$93 \pm 1$
Clays fraction (A02)	$38 \pm 1$	$1.7 \pm 1$	$82 \pm 1$

sample and the A02 clay fraction around 57% of the A50 fraction.

A Gaussian particle size distribution with maximum at 2  $\mu\text{m}$  is observed for the A02 clays fraction. Furthermore cumulative particle size distribution reveal that more than 95% of the sample particles has size smaller than 7  $\mu\text{m}$ . Particle size distribution of the A50 fraction show to maxima at 5 and 30  $\mu\text{m}$ . The first group contains particle size ranging from 2.5 to 20  $\mu\text{m}$  and it represents about 90% of the total amount of A50 fraction the other 10% are particles of size ranging from 20 to 60  $\mu\text{m}$ .

Acid treatment leads to the dissolution of 18% of the clay fraction and the dissolution of the 7% of the A50 fraction. The difference in the dissolution behaviour of the two clays is attributed to their composition and to their particle size. As generally observed, smectite is more sensitive to acid leaching than kaolinite. Moreover for particle of the same composition small particles may

dissolve more readily than the bigger particles.

The dissolution of the clays could be attributed to the leaching of exchangeable ions ( $\text{Mg}^{2+}$ ,  $\text{Ca}^{2+}$ ,  $\text{Na}^+$ ,  $\text{K}^+$ ) and dissolution of hydroxides or carbonates. Many authors (Chritidis et al., 1997; Vincente et al., 1996; Nguetnkam et al., 2005) have shown that destruction of clays structure need concentrated acid solution and longer contact time, than those use herein (that is, 0.5 M hydrochloric acid solution and 48 h contact time).

### X-ray diffraction

XRD patterns of alluvial clay samples show that it consists predominantly in smectite, kaolinite and quartz, with accessory minerals such as anatase, microcline, albite and rutile (Figure 2a). The results of the ethylene glycol test on oriented clay fraction showed the characteristic

displacement of the basal peak of smectite from 15.2 to 18.3 Å (Figure 2b.). The usual displacement of the smectite from 15.2 to 10.1 Å on heating at 550°C is also observed.

All the vertisol profiles in this area showed a similar mineralogical composition; however Nguetnkam et al. (2005, 2007b) found that most of the smectite minerals of the vertisol soil of this zone are mixtures of montmorillonite and beidellite. The spectra of the A50 fraction show a well defined peak of quartz indicating a high amount of quartz in this sample. On the contrary the clay fraction only presents very few amount of quartz. For the acid treated clay, XRD analyses on oriented A02A fraction (Figure 2c) compare well with those of A02 sample, which suggests only limited alteration with 0.5 M HCl.

### Infrared spectroscopy

The infrared spectra of the two clays fractions are presented in (Figure 3). The two spectra have almost the same feature. IR analysis confirms that smectite and kaolinite are the main mineral present in our clay samples. The broad band at  $3390\text{ cm}^{-1}$  is usually attributed to the adsorbed water at the interlayer of smectite clays. The band at  $1612\text{ cm}^{-1}$  is also attributed to smectite interlayer water. This band slightly decreases after acid activation of the clay. The band at  $3698\text{ cm}^{-1}$  is assigned to the OH stretching vibration of kaolinite, whereas the band at  $3620\text{ cm}^{-1}$  is characteristic of the OH stretching of kaolinite and of AlAlOH or AlMgOH groups of smectite. These two bands are not modified by the acid treatment of the clay as already suggested by XRD.

In addition, IR analysis shows the absence of calcium or magnesium carbonates and of organic matter in the studies samples.

### Scanning and transmission electron microscopy

SEM observation on a polish slide of A50 fraction shows large aggregates and small particles dispersed over the entire matrix (Figure 4a). SEM with EDX analysis of the aggregates reveal the presence of smectite [A]: (Si/Al $\approx$ 0.60), of microcline [B]: (Si/Al $\approx$ 2.8 and 3), of quartz [C]: (Al=0), of interstratified [D]: (Si/Al $\approx$ 1.6) and of kaolinite [E]: (Si/Al $\approx$ 2). Those minerals have currently been identified from XRD and IR analyses.

The SEM images of A50 powder shows the usual cluster of rose shaped aggregates of smectite particles (Figure 4b). The TEM observation of crude and acid treated clay fractions (Figure 4c and 4d) suggests that acid attack lead to the fragmentation of large particles into smaller ones, which involve mosaic like platelets and poorly shaped aggregates. TEM-EDX analysis confirms the presence of kaolinite and smectites; they also reveal

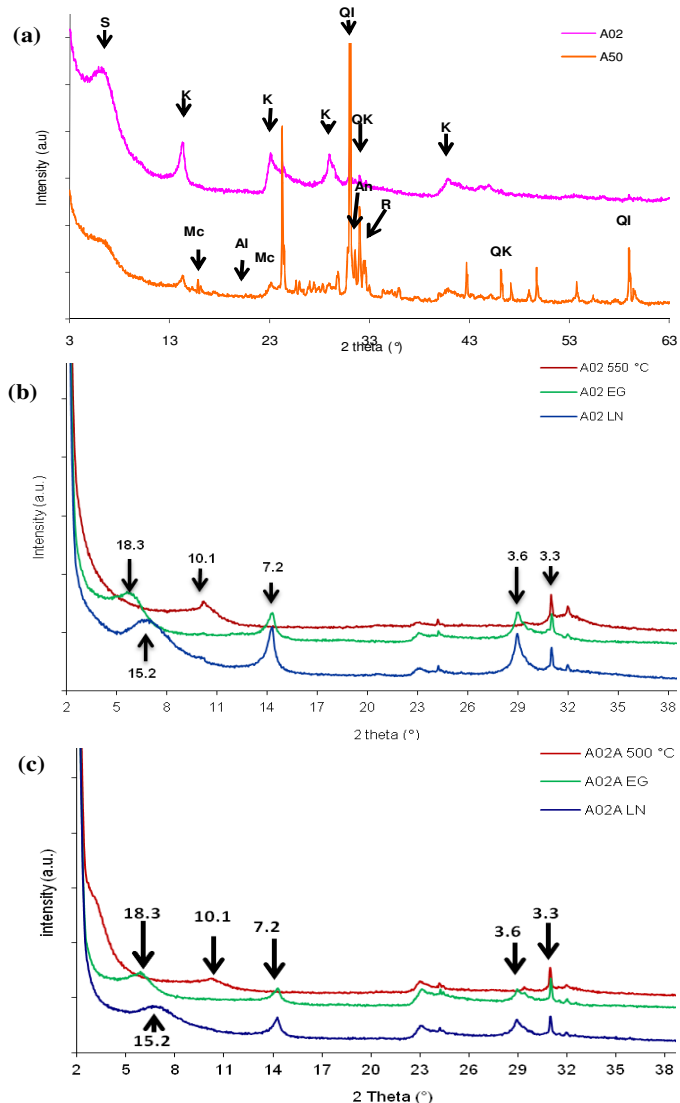


**Figure 2.** X-ray diffraction patterns of a) natural (A02, A50), b) oriented preparation of clay fraction (A02 LN), (A02 EG), (A02 550°C), c) oriented preparation of acidic treatment clay fraction. Basal spacings on Figure1b are given in Å. Nomenclature (S: smectite; K: kaolinite; Mc: microcline; Al: albite; Q: quartz; An: anatase; R: rutile).

the additional presence of quartz, feldspar and iron oxyhydroxides as minor phases.

### Chemical analyses

The mains oxydes of A50 and A02 fractions are  $\text{SiO}_2$ ,  $\text{Al}_2\text{O}_3$  and  $\text{Fe}_2\text{O}_3$  (Table 2). The high amount of  $\text{SiO}_2$  in the A50 fraction is related to its high content in quartz as compare to the clay fraction. Small amount of  $\text{MnO}$ ,  $\text{MgO}$ ,  $\text{CaO}$ ,  $\text{Na}_2\text{O}$ ,  $\text{K}_2\text{O}$ ,  $\text{TiO}_2$  and  $\text{P}_2\text{O}_5$  are also found in the two samples. Acid treatment of the clay leads to the reduction of the amount of  $\text{MgO}$ ,  $\text{CaO}$  and  $\text{Na}_2\text{O}$ . This implied that  $\text{Mg}^{2+}$ ,  $\text{Ca}^{2+}$  and  $\text{Na}^+$  are exchangeable cations of the clays

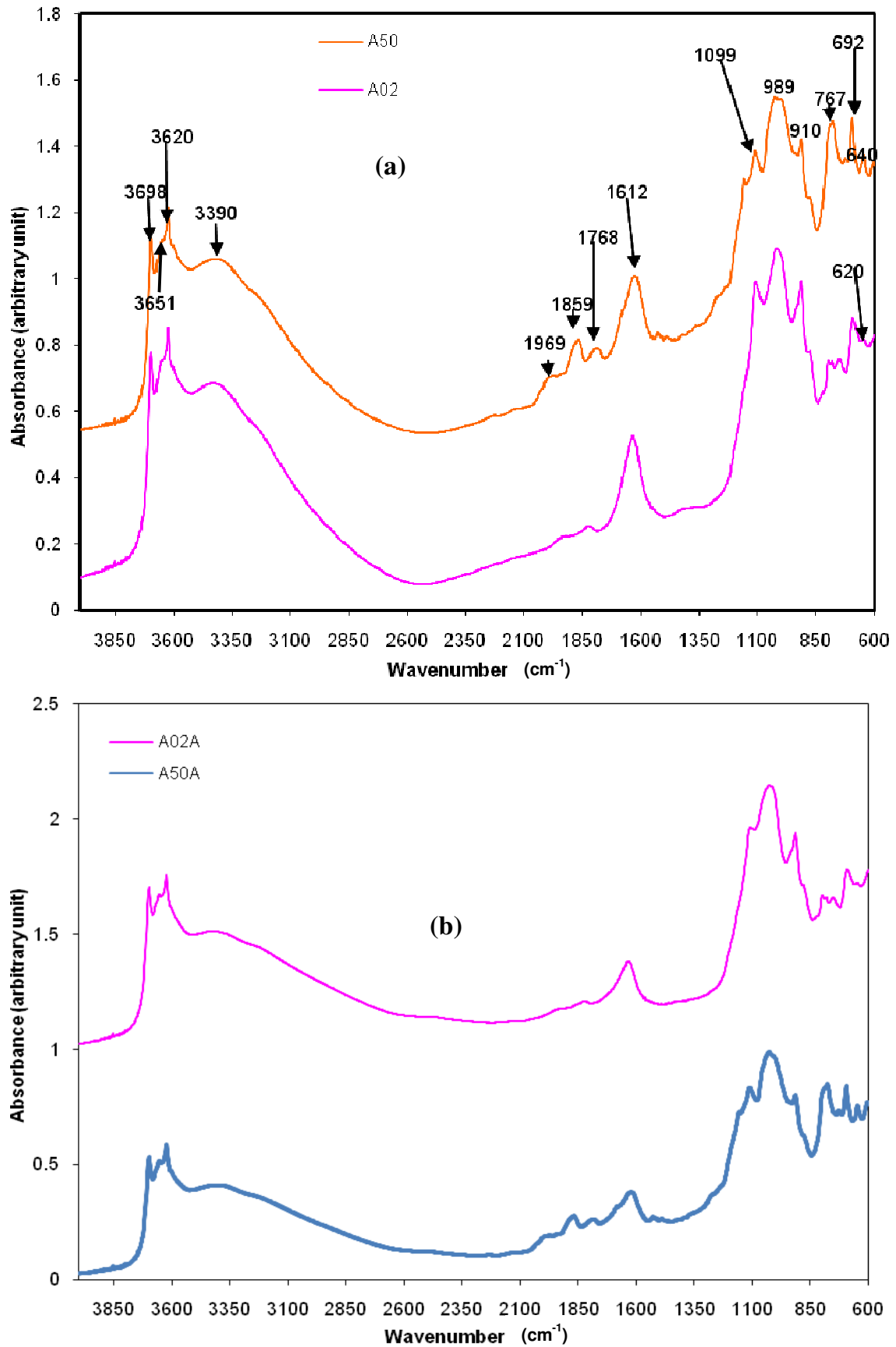
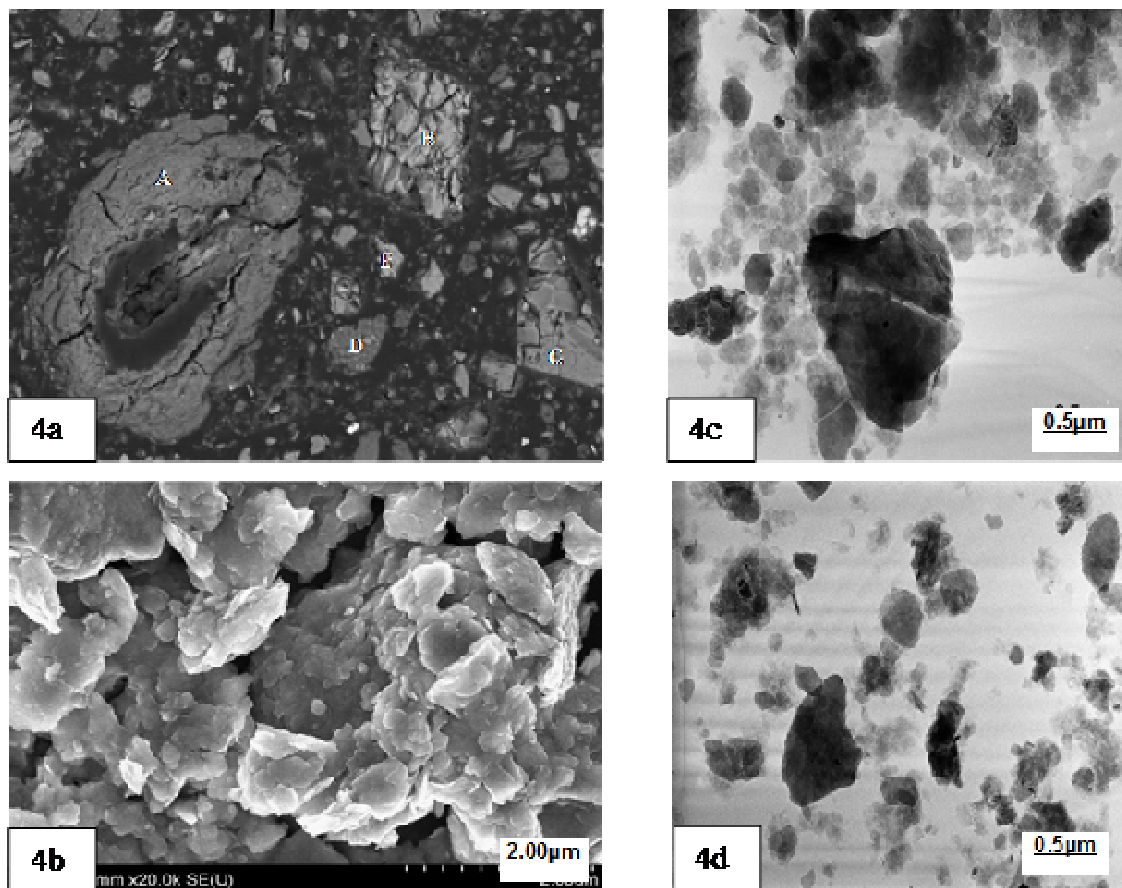


Figure 3. Infrared spectrum of the (a) A02 and A50 and (b) A02A and A50A.



**Figure 4.** Scanning electron photomicrograph (SEM) and TEM micrograph of alluvial clayey fraction, showing typical texture. 4a) SEM A50 (polished slide of clay embedded in resins); 4b) SEM A50 (powder); 4c) TEM A02; 4d) TEM A02A. Minerals identification is derived from EDX analyses.

**Table 2.** Chemical composition of major elements of A50 fraction (<50 μm), and clay fraction (< 2 μm) and the corresponding acid modified sorbents.

Sample(%)	SiO <sub>2</sub>	Al <sub>2</sub> O <sub>3</sub>	Fe <sub>2</sub> O <sub>3</sub>	MnO	MgO	CaO	Na <sub>2</sub> O	K <sub>2</sub> O	TiO <sub>2</sub>	P <sub>2</sub> O <sub>5</sub>	LOI	Total
A02	46.3	22.9	9.2	0.04	1.27	0.87	0.56	1.05	1.26	0.08	16.5	100.0
A02A	47.0	23.4	9.5	0.03	1.01	0.19	0.16	1.01	1.29	0.09	16.3	100.0
A50	60.6	17.0	5.9	0.09	0.75	0.77	0.94	3.18	1.34	0.06	9.45	100.1
A50A	61.9	17.3	5.9	0.06	0.58	0.34	0.77	3.29	1.41	0.06	8.98	100.6

LOI: loss on ignition.

samples. Those cations are exchangeable by H<sup>+</sup>. The contents in Fe<sub>2</sub>O<sub>3</sub>, SiO<sub>2</sub> and the Al<sub>2</sub>O<sub>3</sub> slightly increase after acid treatment. K<sub>2</sub>O<sub>3</sub> decreases slightly in A02A but increases in A50A, showing that potassium is mainly present in feldspar but few amounts are also found in exchangeable position in clays.

The traces elements in Table 3 are observed in this increasing order: Ba, Sr, Zr, Cr, V, Ce, Rb, Zn, La, Ni, Nd, Cu, Ga, Y, Nb, Pb, Th, Co, Pr, Sm, Gd, Dy, U, Be, Cs, Sn, Hf, Er, Yb, Eu, Ta, Ge, W, As, Tb, Ho, Mo, Lu, Tm, Bi, Sb, In. The presence of trace elements in the

studied clays is attributed to substitution, replacement or adsorption of these trace elements on the surface or in the lattices of the studied clay samples (Ekosse, 2000). The global observation is that, the amount of these trace elements cannot reduce significantly the adsorption's capacity of alluvial clay (Ekosse, 2000, 2001).

In general, the behavior of traces is roughly the same for A02 and A50, but the comparison between two samples shows that: Ga, Cr, Cu, La, Be, V, Zn and As are mainly in clay fraction, whereas A50 is enriched in Ba, Ce, Nb, Pb, Rb, Sr, Zr likely in feldspars. The effect

**Table 3.** Trace element analysis of the materials studied (results expressed in ppm; LD = detection limit).

Element	A02	A02A	A50	A50A
As	1.319	1.236	< L.D.	1.233
Ba	717	384.5	1396	1160
Be	4.619	3.452	2.922	2.079
Bi	0.237	0.241	0.222	0.237
Cd	< L.D.	< L.D.	< L.D.	< L.D.
Ce	120.5	113.5	161.8	156.3
Co	19.6	17.77	18.74	12.61
Cr	134.4	137.4	104	106.7
Cs	4.581	4.628	3.213	3.312
Cu	39.95	35.39	29.62	24.15
Dy	6.613	5.456	7.098	5.391
Er	3.279	2.751	3.725	2.965
Eu	2.403	1.955	2.386	1.71
Ga	34.97	35.77	24.01	24.16
Gd	8.491	6.781	8.645	6.181
Ge	1.826	1.884	1.392	1.468
Hf	3.644	3.81	8.821	8.957
Ho	1.193	0.981	1.32	1.031
In	0.109	< L.D.	< L.D.	< L.D.
La	75.82	64.76	67.14	51.39
Lu	0.497	0.416	0.565	0.48
Mo	0.887	1.052	0.782	0.785
Nb	28.25	28.25	29.24	30.45
Nd	61.27	50.48	59.46	42.33
Ni	62.62	61.77	42.77	36.48
Pb	25.977	22.5792	37.105	32.614
Pr	16.78	13.93	15.87	11.67
Rb	104.8	105.4	130	134.6
Sb	0.213	0.233	0,236	0.234
Sm	11.24	9.192	11	7.799
Sn	4.207	4.338	3.329	3.364
Sr	156.6	76.36	244.9	200.1
Ta	2.145	2.2	2.312	2.439
Tb	1.212	0.989	1.265	0.927
Th	20.28	20.47	22.58	24.32
Tm	0.479	0.397	0.547	0.455
U	5.146	3.968	5.197	4.2
V	130	121.9	106.2	106
W	1.47	1.531	1.399	1.502
Y	34.66	27.86	37.87	28.59
Yb	3.188	2.676	3.68	3.073
Zn	103.6	96.45	77.15	53.75
Zr	137.2	141.1	342	340.6

LD is 1% for oxides; for traces, it is 5% of values above 100 ppm, 10% in the vicinity of 50 ppm and can reach 50% to 10 ppm.

of acid leaching shows that Ga, Cr are located in clay structure whereas Ba, Cu, La, Be, Sr, V, Zn and As are found in exchangeable position. Concerning acid treat-

ment Pb, Zn, and Cu are slightly leached while Cr, Co, Ni and Sn are resistant.

### Physico-chemical characteristics of the alluvial clayey soil from Far North Cameroon

The cation exchange capacity (CEC) values measured from variation in concentration of cobaltihexamine match those deduced from the chemical analysis of exchangeable cation for all the samples described herein. This confirms the absence of soluble phases in the studied fraction.

The CEC of the clay fraction (Table 4) lie between the values reported in the literature for smectite that is 60 to 150 meq/100 g (Tsai et al., 2002). The lower CEC value for A50 fraction compared to clay fraction correlates with its lower content in clays. Indeed, the CEC ratio between A50 and A02 is 0.54, in good agreement with the 57% of clays in A50. From the analyses of the cations exchanged with cobaltihexamine, it can be concluded that around 2/3 of the layer charge is compensated by divalent cations ( $\text{Ca}^{2+}$  and  $\text{Mg}^{2+}$ ).

The cation exchange capacities of activated clay are much lower 60% than those of the initial sample. This is due to replacement of exchangeable cation by  $\text{H}^+$  ion. Of course it is observed that  $\text{Na}^+$ ,  $\text{Ca}^{2+}$ ,  $\text{Mg}^{2+}$  concentration obtains on activated clay represented roughly 1/3 of their respective initial concentration. The observed decrease in CEC can be assigned to a decrease in swelling capacities of  $\text{H}^+$  with migration into interlayers (Komadel et al., 2005).

### Textural properties

The adsorption-desorption isotherms on the four samples are reported in Figure 5 are typical of clay materials containing smectites (Neaman et al., 2003). Numerical values deduced from the adsorption and desorption isotherm are given in Table 5. The difference in the specific surface areas (SSA) of A02 and A50 fractions can be attributed to their quartz content. In fact A50 fraction has contains a large amount of quartz, and quartz particles present low specific surface areas compared to clays. Indeed, the 0.54 SSA ratio between A50 and A02 samples is also consistent with CEC and clay content of A50 showing that sandy fraction of A50 has no surface area. Microporosity represent about 20% of the total surface area and can be assigned to clay layers organisation as it is generally observed in the case of swelling clays with divalent exchangeable cations (Neaman et al., 2003).

Treatment of the clays with 0.5 M HCl does not modify significantly the textural properties of the clays. Many authors (Nguetnkam et al., 2005; Van Rompay et al., 2002; Komadel et al., 1996; Madejova et al., 1992) observed

**Table 4.** Equilibrium pH, cation exchange capacities (CEC), and exchangeable cations of the clay fraction.

Sample	pH $\pm 0.1$	CEC (chem) meq/100 g $\pm 5$	CEC (UV) meq/100 g $\pm 5$	Na <sup>+</sup> (meq/100 g) $\pm 2$	K <sup>+</sup> (meq/100 g) $\pm 1$	Ca <sup>2+</sup> (meq/100 g) $\pm 2$	Mg <sup>2+</sup> (meq/100 g) $\pm 1$
A02	9.2	58	62	14.8	1.5	29.2	13.0
A50	9.5	31	34	6.3	0.6	15.8	6.3
A02A	5.0	21	24	4.7	0.4	10.6	4.6

Chem: derived from chemical analysis of displaced cations. UV: derived from the measurement of cobaltihexamine concentrations by UV-visible spectroscopy.

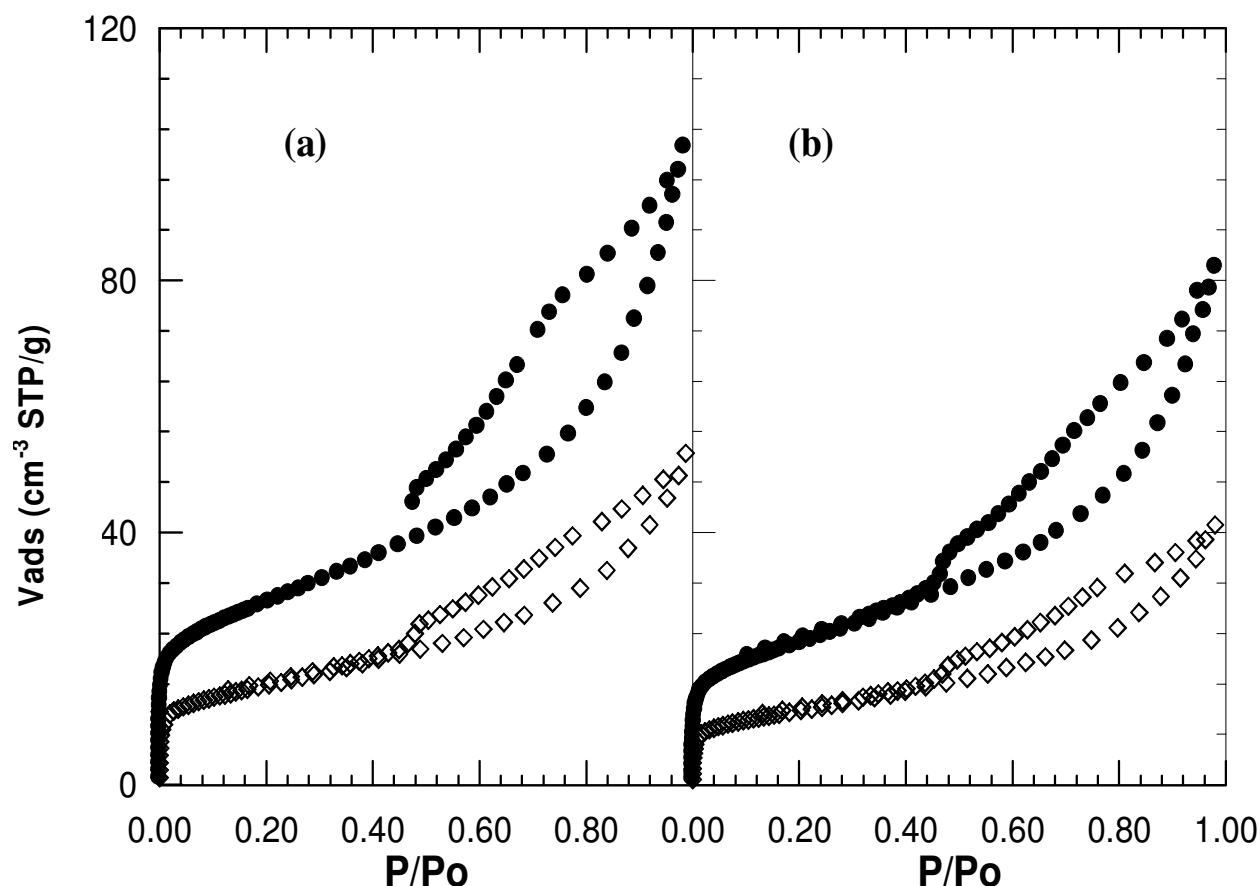


**Figure 5.** Nitrogen adsorption and desorption isotherms at 77K. for a) clay fraction (A02) and sandy fraction (A50), b) acidic treatment clay fraction (A02A) and sandy fraction (A50A). ●: A02; ◇: A50.

the increase of the surface area and the micropore volume on acid treatment of smectite like clays; they attributed those phenomena to the formation of free silica due to partial destruction of clay structure. However those authors used acid solution of higher concentration and a longer contact time than those use in this work.

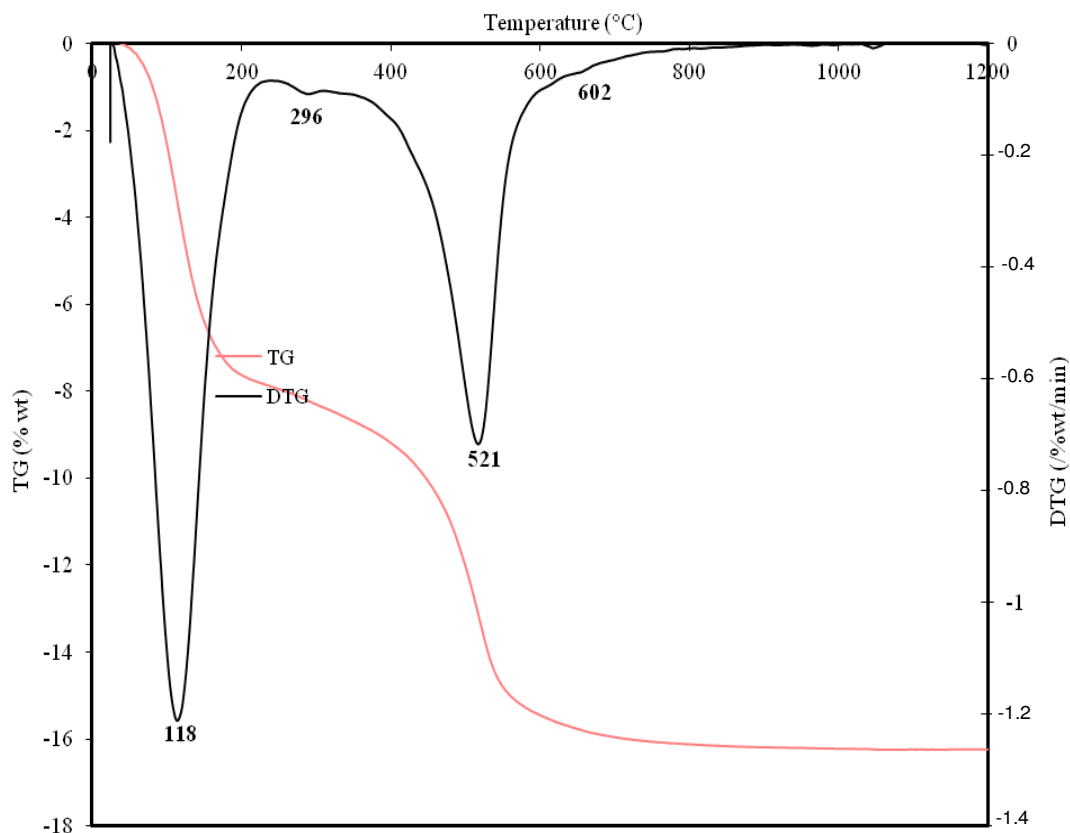
### Thermal analysis

DTG curves shows two main endothermic peak (Figure 6). The first peak between 40 and 200 °C corresponds to

the dehydration of smectite. The second peak between 300 and 700 °C with maximum at 520 °C correspond to the dehydroxylation of kaolinite and smectite minerals. This result is confirmed on the TG curves on which there are two important weight loss (who have the same amount 8.0% for A02) between 90 °C and 300 °C for hydration water and between 400 and 650 °C for clay dehydroxylation. The minor peak at 296 °C confirms the presence of iron oxy-hydroxides as already observed by electron microscopy. Estimation of clay amount in A50 obtained from weight loss ratio between A02 (8.0%) and A50 (4.7%) is 59%  $\pm$  5%.

**Table 5.** Textural parameters deduced from N<sub>2</sub> adsorption desorption isotherms (SSA: specific surface area).

Sample	BET C constant	BET SSA (m <sup>2</sup> /g) ± 1	Non microporous surface area (m <sup>2</sup> /g) ± 1	Microporous equivalent surface area (m <sup>2</sup> /g) ± 1	Microporous volume (cm <sup>3</sup> /g) ± 0.0003
A02	215	103	82	26	0.0091
A02A	162	101	82	22	0.0076
A50	337	56	44	15	0.0053
A50A	239	52	42	12	0.0042

**Figure 6.** Thermogravimetric and differential thermogravimetric analyses of an alluvial clayey: (A02).

### Structural formula of an alluvial clayey soil from Far-North of Cameroon

The previous characterization analyses show consistent results for the content of clay in the A50 sample. Indeed results derived from the particle size separation has a yield of 57%, whereas BET, CEC and thermal analysis give 54, 55 and 59% respectively.

The agreement of the results indicates that the clay fraction A02 extracted from the sample A50 is representative of the entire clay fraction initially present. The quantitative mineralogical study of the clay fraction A02 can give an objective estimate in the content of the reactive fraction of the sample. Thus the reactive fraction

of the studied alluvial clay (A02) is mainly composed of disordered kaolinite and interstratified smectite / kaolinite. Its surface area is 104 m<sup>2</sup>/g and its CEC is 62 meq/100 g. Quantitative mineralogical analysis of the sample of the reactive fraction may be derived from TEM. The atomic percentages of elements obtained from the EDS analyses coupled with the TEM images permit to calculate the Si/Al ratio and also to identify the different phases present in the alluvial clay. The obtained analyses are plotted in a Al-Si-Fe ternary diagram (Figure 7) which highlights the presence of some accessory minerals and shows that all clay particle analyses are spread on a mixture straight line, between kaolinite pole and smectite pole. These analyses allow us to propose a structural

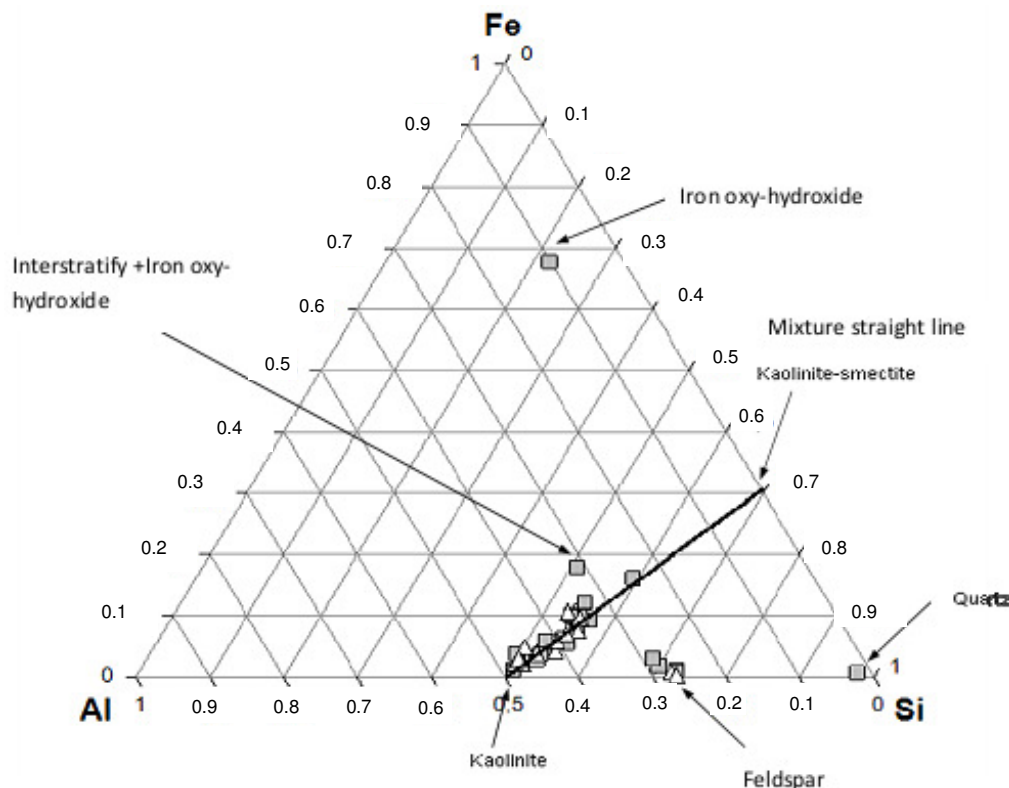


**Figure 7.** Al-Si-Fe ternary diagram elemental analyses obtained by EDS in TEM on particulate samples A02 ( $\Delta$ ) and A02A ( $\blacksquare$ ).

formula for kaolinite:  $\text{Si}_2\text{Al}_{1.95}\text{Fe}_{0.05}\text{O}_5(\text{OH})_4$ , with significant iron content which is in agreement with the disorganized nature observed by infrared spectroscopy. Assuming that the reference smectite pole on the Al-Si-Fe ternary diagram is pure and contains no kaolinite, smectite structural formula can be calculated is:  $[\text{Si}_{3.42}\text{Al}_{0.58}]_{\text{tetra}}[\text{Al}_{0.87}\text{Fe}_{0.96}\text{Mg}_{0.17}]_{\text{octa}}\text{O}_{10}(\text{OH})_2(\text{C}^+)_{0.75}$ .

The calculated smectite has a double character beidellite-smectite with tetrahedral charge of 0.58 greater than the octahedral charge of 0.17. Its calculated weightloss and CEC are 4.5% and 186 meq/100 g, respectively. From structural, CEC and chemical analyses, it can be concluded that all the calcium and sodium of A02 are in exchangeable position whereas 75% of Mg is in octahedral position and less than 10% of K is exchangeable. This smectite can then be considered as a high charge smectite with limited swelling capacities due to the presence of non-swelling layers with dehydrated  $\text{K}^+$  interlayers as already observed by Mosser-Ruck et al., (2001) for other high charge smectites.

From the elemental compositions of kaolinite and smectite endmembers, it is possible to calculate the percentage of these two phases in mixed particules. Figure 8 shows the frequency distribution obtained from 27 particles in both samples A02 and A02A. It follows

from this observation that there is a family with around 20% smectite and a family with a wide kaolinite/smectite distribution centered at around 50% of smectite.

The structural formulas of smectite and kaolinite being established, it is possible to estimate their quantitative proportions (Table 6) by making the assumption that the feldspar and iron oxy-hydroxide are negligible in quantity, which is not the case for quartz visible by XRD. Least squares estimation of quartz, kaolinite and smectite was carried out from the contents in Si, Al, Mg and Fe of the chemical analysis of Table 2. The results obtained are shown in Table 6 with an error margin of 3 to 5% for quartz, kaolinite and smectite. At this stage, it is not possible to clearly make the differences between pure kaolinite and kaolinite in mixed-layer kaolinite-smectite particles.

The estimated weight for dehydroxylation of the mixture is 7.3% which is consistent with the results of TG in the range of 8.0%. Theoretical CEC of dehydrated product is 96 meq/100 g which is well above the CEC measured around 62 meq/100 g (Table 3).

This last result confirms that there are non-swelling layers in A02 as suggested by the strong structural charge calculated for the smectite pole on the ternary diagram. The CEC ratio shows that the percentage of non-swelling layers is about 35%.

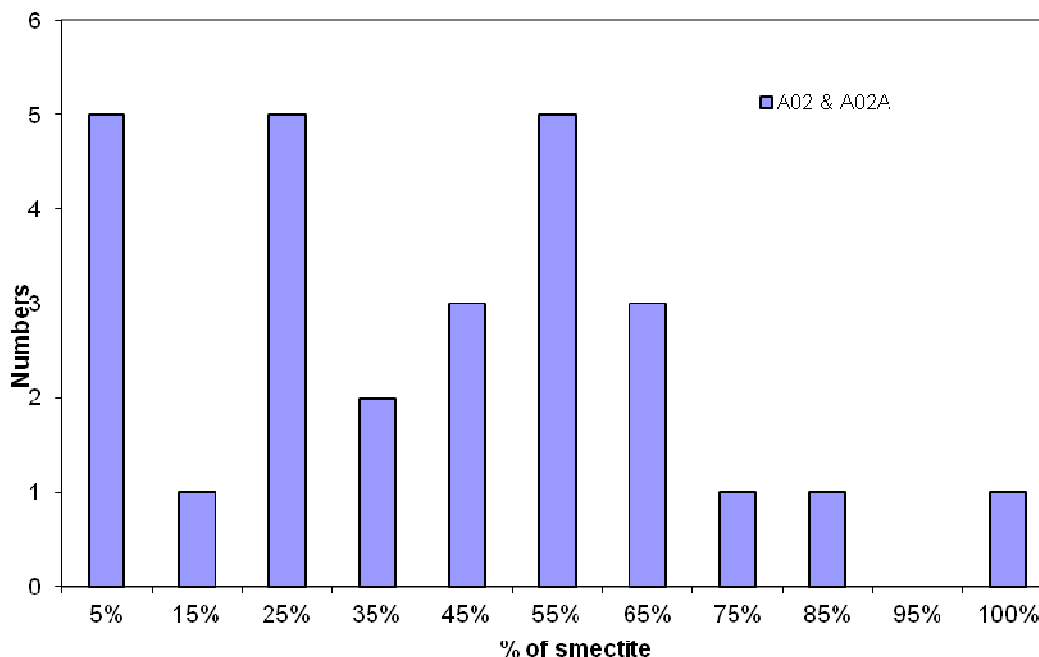


Figure 8: Frequency Distribution of the clay family.

Table 6. Proportion of quantitative mineralogical phases present in the alluvial clay.

A02	Mass (%)
Quartz	5
Kaolinite	38
Smectites	46
TiO <sub>2</sub>	1
Others	1
hydration	9
Total	100

## DISCUSSION

DRX spectra of activated clays indicate that acid leaching affects the (001) line of clay minerals and results in intense partial structural modifications. No additional crystalline phase is observed in reaction products suggesting that crystalline disorder is accompanied by the formation of amorphous phases.

After mild acid activation of alluvial clay, the structural OH stretching vibrations of the different clay do not present any significant changes whereas the signal vOH around 3390 cm<sup>-1</sup> corresponding to adsorbed water widens. In parallel, the 1612 cm<sup>-1</sup> band, corresponding to the δOH vibration of water, suggesting the decrease of the amount of swelling clays. The 1099 and 1020 cm<sup>-1</sup> bands (δSi-O of the silicate network of clays) widens while the signal at 692 cm<sup>-1</sup> (Si-O-Al) decreases with acid

concentration. These features suggest that the tetrahedral sheets are attacked during acid activation. The 910 cm<sup>-1</sup> band (deformation δOH of AlAl-OH) decreases. In a similar way, the 880 cm<sup>-1</sup> band (deformation δOH of AlFe-OH) becomes very diffuse with the increase in acid concentration. These two observations indicate that the octahedral layers are also attacked during acid activation. The progressive widening of the 1099 and 1020 cm<sup>-1</sup> bands coupled to the appearance of a 3698 cm<sup>-1</sup> band (elongation vibration vOH of free Si-OH groups) and the increase of the 767 cm<sup>-1</sup> band indicate the formation of amorphous silica. (Rhodes and Brown, 1992; Breen et al., 1995; Suárez Barrios et al., 1995; Vicente et al., 1996; Christidis et al., 1997; Falaras et al., 1999).

SEM micrographs of acid activated clays reveal small corroded particles. Electron diffraction images carried out by TEM clearly show that activated clays are very poorly crystallized and can be classified as amorphous materials as the diffraction rings visible for natural clays are not observed anymore after acid activation.

Results concerning chemical analysis obtained after acid activation reveal:

- (i) a strong reduction in both CaO and Na<sub>2</sub>O.
- (ii) an average and gradual reduction in MgO and K<sub>2</sub>O.
- (iii) a weak and gradual reduction in Al<sub>2</sub>O<sub>3</sub> and Fe<sub>2</sub>O<sub>3</sub>.
- (iv) a relative increase in SiO<sub>2</sub>.

The decrease of both CaO and Na<sub>2</sub>O suggests a removal of the exchangeable cations Ca<sup>++</sup> and Na<sup>+</sup> from interlayer

spaces. The reduction in octahedral oxides ( $\text{Al}_2\text{O}_3$ ,  $\text{MgO}$  and  $\text{Fe}_2\text{O}_3$ ) and the concomitant increase in silica confirm that the original structure of clay is partially significantly modified. The weak decrease in  $\text{K}_2\text{O}$  content could be assigned to the presence of feldspars.

The decreasing of C constant is in good agreement with the formation of low energy surfaces, such as amorphous silica. The microporosity derived from t-plot displays only marginal variations, independent of the concentration in acid. It can then be concluded that acid leaching does not generate any micropores and that precipitated silica is not microporous. Evolution is different for mesoporosity that increases regularly with acid concentration suggesting that precipitated silica is mesoporous, as generally observed for amorphous silica gels.

The CEC data given show a decrease in the CEC of activated clays. The distribution of exchangeable cations in activated samples confirms their removal upon acid treatment. This is particularly striking in the case of  $\text{Ca}^{2+}$ , which is the major cation in non-treated samples. In the initial samples, CEC values measured from variations in concentration of cobaltihexamine match those deduced from the chemical analysis of exchanged cations. This is no longer true in activated samples; such behaviour can be assigned to the presence of exchangeable  $\text{H}^+$  ions as suggested by the pH values of the samples. Such results then confirm that upon acid activation, most interlayer cations are replaced by  $\text{H}^+$  ions.

The crystal chemistry and physical chemistry of the analysed samples show that acid activation results in a partial destabilization of the clay followed by the precipitation of an amorphous compound mainly siliceous.

## Conclusions

This work has focused on studies related to mineralogical and physico-chemical properties of alluvial clays from far-north region of Cameroon via chemical, structural and textural analyses.

The main minerals present in this clay are smectite (high-charge beidellite), kaolinite, and quartz. Accessory minerals found are iron oxy-hydroxide, anatase, microcline, albite and rutile. The textural and surface charge of alluvial clay matches those of smectite mineral. Previous works of Ekodeck (1976) and Nguetnkam et al. (2005, 2007b) showed that 2:1 clays are the main minerals in the Vertisols of the region of the far north of Cameroon. The studied clay thus has properties consistent with these previous works.

Smectites, because of their swelling properties and cation exchange capacity, are among the most commonly used mineral for adsorption of dissolved compounds in solution and it is then hoped that the alluvial clay of the extreme Northern Cameroon by its overall negative surface charge and its low mobility of heavy metals

naturally present in the sample can be used for the adsorption of heavy metals from waste water of Cameroon.

Nevertheless, a mild acid treatment shows that Acid treatment of alluvial clay results in the classically crystallochemical and textural modifications: partial destruction of the original clay structure, replacement of the interlayer cations by  $\text{H}^+$ , removal of octahedral cations, dissolution of the tetrahedral sheets, and formation of an amorphous silica. Concomitantly, the CEC progressively decreases while the specific surface area and mesoporosity of the studied materials increase. But acid leaching of Cameroonian clays does not generate any micropores. Smectites are more sensitive to acid leaching than kaolinite. Therefore, activated Cameroonian alluvial clays also might be expected to perform well in respect with depollution of waste water. Work is in progress to verify the effective adsorption capacity of the activated and pure Cameroonian alluvial clays by using the treated series for the depollution of micro-industries waste water.

## ACKNOWLEDGMENT

Henriette ZANGUE ADJIA's thesis received financial support from the "Service de la Coopération et d'Action Culturelle (SCAC)" through French Embassy in Cameroon via an EGIDE scholarship.

## REFERENCES

- Alther GR (1999). Removal of oil from wastewater with organo clay. *Int. Water Irrig. Rev.* 19:44.
- Bike Mbah JB, Kamga R, Nguetnkam JP, Fanni J (2005). Adsorption of pigments and free acids from shea butter on activated Cameroonian clays. *Eur. J. Lipid Sci. Technol.* 107(6):387-394.
- Bitom D, Volkoff B, Abossolo-Angue M (2003). Evolution and alteration *in situ* of a massive iron duricrust in Central Africa. *J. Afr. Earth Sci.* 37:89-101.
- Breen C, Madejova J, Komadel P (1995). Characterization of moderately acid-treated, size-fractionated montmorillonites using IR and MASNMR spectroscopy and thermal analysis. *J. Mater. Chem.* 5:469-474.
- Christidis GE, Scott PW, Duhnam AC (1997). Acid activation and bleaching capacity of bentonites from the islands of Milos, Chios, and Aegan. *Appl. Clay. Sci.* 12:329-347.
- Davies ED, Nustrat J (2002). The adsorption of herbicides and pesticides on clay minerals and soils - Part I: Isoproturon. *J. Inclusion Phenom. Macrocycl. Chem.* 43:329-336.
- Davies ED, Nustrat J (2003). The adsorption of herbicides and pesticides on clay Minerals and soils - Part II: Atrazine. *J. Inclusion Phenom. Macrocycl. Chem.* 46:57-64.
- De Boer JH, Linsen BG, Osinga TJ (1996). Studies on pore systems in catalysts - Part VI: The universal curve. *J. Catal.* 4:643-648.
- Djoufac W, Kamga R, Figueras F, Njopwouo D (2007). Acid activation and bleaching capacity of some Cameroonian smectite soil clays. *Appl. Clay Sci.* 37:149-156.
- Ekodeck GE (1976). Contribution à l'étude de la nature et du comportement géotechnique des dépôts superficiels gonflants du Nord Cameroun. Thèse 3ème cycle, Sci. Ter. Université de Grenoble p. 181.
- Ekosse G (2000). The Makoro kaolin deposit, south eastern Botswana: Its genesis and possible industrial applications. *Appl. Clay Sci.* 16:

- 301-320.
- Ekosse G (2001). Provenance of the Kgwakgwa kaolin deposit in southeastern Botswana and its possible utilization. *Appl. Clay Sci.* 20:137-152.
- Era-Cameroun (2002). Mise en place des structures de pré-collecte et de traitement des déchets solides urbains dans une capitale tropicale: Le cas de Yaoundé-Cameroun. Rapport final.
- Espantaléon AG, Nieto JA, Fernandez M, Marsal A (2003). Use of activated clays in the removal of dyes and surfactants from tannery waste waters. *Appl. Clay Sci.* 24:105-110.
- Falaras P, Kovanis I, Lezou F, Seiragakis G (1999). Cottonseed oil bleaching by acid activated montmorillonite. *Clay Miner.* 34:221-232.
- Kamga R, Kayem JG, Rouxhet PG (2000). Adsorption of Gossypol from Cotton seed oil on oxides. *J. Coll. Interf. Sci.* 232:198-206.
- Komadel P, Madejova J, Janek M, Gates WP, Kirkpatrick RJ, Stucki JW (1996). Dissolution of hectorite in inorganic acids. *Clays Clay Miner.* 44:228-236.
- Komadel P, Madejova J, Bujdák J (2005). Preparation and properties of reduced-charge smectites - A review. *Clays Clay Miner.* 53(4):313-334.
- Lumdsen DG, Evans LJ, Bolton KA (1995). The influence of pH and chloride on the retention of cadmium, lead, mercury and zinc by soils. *J. Soil Contam.* 4:137-150.
- Madejova J, Komadel P, Cícel B (1992). Infrared spectra of some Czech and Slovak smectites and their correlation with structural formulas. *Geol. Carpathica-Ser. Clays: Bratislava (Czechoslovakia)* 1:9-12.
- Maqueda C, Morillo E (2001). Sorption of chlormequat on montmorillonite as affected by dissolved copper. Influence of background electrolytes. *Clay Miner.* 36:473-481.
- Mosser R, Pironon J, Cathelineau M, Trouiller A (2001). Experimental illitization of smectite in a K-rich solution. *Eur. J. Miner.* 13(5):829-840.
- Neaman A, Pelletier M, Villieras F (2003). The effects of exchanged cation, compression, heating and hydration on textural properties of bulk bentonite and its corresponding purified montmorillonite. *Appl. Clay Sci.* 22(4):153-168.
- Nguetnkam JP, Kamga R, Villieras F, Ekodeck GE, Yvon J (2007a). Altération du granite en zones tropicales: Exemple de deux séquences étudiées au Cameroun (Afrique). *Etude et gestion des sols* 14:31-41.
- Nguetnkam JP, Kamga R, Villieras F, Ekodeck GE, Yvon J (2007b). Pedogenic formation of smectites in a vertisol developed from granitic rock from Kaélé (Cameroon, Central Africa). *Clays Miner.* 42:487-501.
- Nguetnkam JP (2004). Les argiles des vertisols et des sols fersiallitiques de l'extrême Nord Cameroun: Genèse, propriétés cristalochimiques et texturales, typologie et applications à la décoloration des huiles végétales. Thèse Doctorat d'Etat, Université de Yaoundé I p. 216.
- Nguetnkam JP, Kamga R, Villieras F, Ekodeck GE, Razafitianamaharavo A, Yvon J (2005). Assessment of the surface areas of silica and clay in acid-leached clay material using concepts of adsorption on heterogeneous surfaces. *J. Coll. Interf. Sci.* 289:104-115.
- Pialy P, Njopwouo D, Bonnet JP (2009). Étude de quelques matériaux argileux du site de Lembo (Cameroun) : Minéralogie, comportement au frittage et analyse des propriétés d'élasticité. Thèse de Doctorat à ENSCI Limoges (France) p. 147.
- Rhodes CN, Brown DR (1992). Structural characterization and optimization of acid treated montmorillonite and high-porosity silica supports for ZnCl<sub>2</sub> alkylation catalysts. *J. Chem. Faraday Trans.* 88(15):2269-2274.
- Robertson A, Dodgson J, Gormley IP, Collings P (1982). An investigation of the adsorption of oxides of nitrogen on respirable mineral dusts and the effects on their cytotoxicity. In: Walton, W.H. (Ed.), *Inhaled Particles V*. Pergamon Press, Oxford pp. 607-622.
- Shawabkeh RA, Tutunji MF (2003). Experimental study and modeling of basic dye sorption by diatomaceous clay. *Appl. Clay Sci.* 24:111-120.
- Suárez Barrios M, Robert M, Elsass F, Martin Pozas JM (1995). Evidence of a precursor in the neoformation of palygorskite. New data by analytical electron microscopy. *Clay Miner.* 29:255-264.
- Tsai WT, Hsieh MF, Sun HF, Chien SF, Chen HP (2002). Adsorption of paraquat onto activated bleaching earth. *Bull. Environ. Contam. Toxicol.* 69:189-194.
- Van Rompay K, Van Ranst E, De Coninck F, Vindevogel N (2002). Dissolution characteristics of hectorite in organic acids. *Appl. Clay Sci.* 21:241-256.
- Vicente Rodriguez MA, Suarez M, Lopez Gonzalez JD, Banares Munoz MA (1996). Characterization, surface area and porosity analyses of the solid obtained by acid leaching of a saponite. *Langmuir* 12:566-572.
- Worral F, Parker A, Rae JE, Johnson AC (1996). Equilibrium adsorption of isoproturon on soil and pure clays. *Eur. J. Soil. Sci.* 47:265-272.
- World Bank (1992). *Rapport sur le Développement dans le Monde. Le développement et l'environnement*. Washington DC.
- Wu J, Laird DA, Thompson ML (1999). Sorption and desorption of copper on soil clay components. *J. Environ. Qual.* 28:334-338.
- Yvon J, Cases JM, Villieras F, Michot L, Thomas F (2002). Les minéraux techniques naturels: Connaissance, typologie et propriétés d'usage. *Cr. Acad. Sci. Géosci.* 334:717-730.